Received: 31 October 2022 | Revised: 13 January 2023 | Accepted: 22 January 2023

DOI: 10.1111/ffe.13966

ORIGINAL ARTICLE

FFEMS Fatigue & Fracture of Engineering Materials & Structures

WILEY

Fatigue life of unidirectional 90° carbon/epoxy laminates made of conventional and ultra-thin plies varying manufacturing and testing conditions

Serafín Sánchez-Carmona | **Elena Correa** | **Alberto Barroso** | **Federico París**

Group of Elasticity and Strength of Materials, Department of Continuum Mechanics and Theory of Structures, School of Engineering, Universidad de Sevilla, Seville, Spain

Correspondence
Serafín Sánchez-Carmona, Group of Elasticity and Strength of Materials, Department of Continuum Mechanics and Theory of Structures, School of Engineering, Universidad de Sevilla, 41092, Seville, Spain.
Email: sscarmona@us.es

Funding information
Universidad de Sevilla, Grant/Award Number: VIPPIT-2018-II.2; Consejería de Economía y Conocimiento, Junta de Andalucía, Grant/Award Number: P18-FR-3360; Spanish Ministry of Science, Innovation and Universities, Grant/Award Number: PID2021-126279OB-I00

Abstract

Unidirectional 90° laminates (UD-90) have been tested under tension–tension loading ($R = 0.1$) to comprehend the effect of different conditions on their fatigue life. Four different case studies have been evaluated: the existence of porosity using two different UD-90 laminates cured at different pressures in an autoclave, the importance of the surface finishing when a pressure plate is used, the effect of load frequency, and the relevance of the prepreg thickness comparing 190 and 50 g/m^2 prepregs while keeping the total thickness of the laminates constant. All these case studies have been analyzed employing *S–N* curves as the starting point of the authors' current research for the prediction of the onset of transverse damages in ultra-thin plies in the assessment of different cross-ply laminates under cyclic loading.

KEYWORDS

composites, fatigue analysis, fiber/matrix failure, mechanical testing, tensile mechanical properties, ultra-thin prepreg

Highlights

- Ultra-thin plies motivate this work to look into *scale effect* under fatigue.
- 90° unidirectional laminates are tested under tension–tension fatigue loading.
- Conventional (190 g/m^2) and ultra-thin (50 g/m^2) carbon/epoxy prepregs are used.
- *S–N* curves are obtained at different cyclic loading conditions without losing accuracy.

1 | INTRODUCTION

The fatigue behavior of any material is a relevant issue due to its cyclic load environment when they are under service. For instance, aircraft suffer fatigue loads when flying, and the wind turbine blades are constantly subjected to rotative cyclic loads. For that reason, composite materials' fatigue life is a continuously updating research area. Due to the enormous number of possibilities when composite material is used, many issues have to be considered if an accurate assessment wants to be achieved. As many authors expounded in Harris,[1] fatigue failure on composite materials depends on material features and testing conditions due to the accumulation of different damages, such as fiber/matrix debonding, matrix cracking, delaminations, splitting, and fiber breakage. On the one hand, composite type, stacking sequence, lay-up manufacture, ply thicknesses, and position, among other material features, need to be considered to precisely assess fatigue life. And, on the other hand, loading type, stress ratio, stress levels, and frequency, among others testing conditions, must be taken into account to efficiently analyze the fatigue behavior of composite materials.

Over the last four decades, several research groups have looked into different combinations of material features and testing conditions. There are some studies, see for instance, previous studies,[2-7] that have employed unidirectional composite materials to assess different fatigue case studies. These works have aimed to understand how simple material configurations behave as a first step to comprehend the performance of more difficult stacking sequences. Many other researchers have used complex composite material configurations to directly analyze how fatigue behavior develops according to these particular material features. In order to show the multiple combinations in different research works over the last decades, some studies have been selected. Previous studies[8-18] have a common feature in their work, all of them mainly study cross-ply laminates. However, each piece of work analyzes different material features and testing conditions. Whereas Gamstedt and Sjögren,[12] Berthelot and Le Corre,[13] and Carraro et al.[17] deal with glass fiber reinforcements, the rest of them deal with carbon ones. All of them work with thermoset resins, epoxy mainly, except Henaff-Gardin and Lafarie-Frenot[10] who also treat thermoplastic matrices. A similar case occurs when loading type is considered, as all of them analyze the fatigue behavior under uniaxial loads, except Tohgo et al.[15] who studies it under multiaxial loading. Other studies deal with different stacking sequences covering very diverse materials and testing features as expounded before for cross-ply laminates. For instance, previous studies,[19–26] among others, have analyzed the fatigue behavior of quasi-isotropic and/or angle-ply laminates.

According to lay-up manufacture, any configuration may imply voids and its quantity mainly depends on the curing method. As Sisodia et al.[25] and El-Dessouky and Lawrence[27] have expounded, porosity is a detrimental and hard-damaging effect on the fatigue performance of composite materials. Hence, it is worth analyzing the minimum quantity of porosity that can be produced after curing in an autoclave to consider it, avoiding any detrimental effect on fatigue performance.

Another important feature to take into consideration is the ply thickness. During the last decades, a phenomenon related to this parameter, the *scale effect*, has been studied by the scientific community. Many researchers have experimentally assessed the influence of the thickness of the weakest lamina under quasi-static load although few of them have used ultra-thin plies. Recently, París et al.[28,29] have physically explained the *scale effect* based on the damage mechanisms involved in quasi-static failure after a wide variety of experimental programs and numerical correlations, demonstrating that the first damage in the weakest lamina is delayed as long as its thickness decreases and expounding the change in the quasi-static damage mechanisms. However, few researchers have micromechanically looked into this phenomenon under cyclic loading. Some studies, such as Sihn et al.[22] and Kötter et al.,[30] among others, have provided some encouraging improvements related to better fatigue performance macroscopically when ultra-thin plies are involved in the manufacturing process of composite laminates. These studies, among others, have been well reviewed by Galos[31] both under static and fatigue testing.

Among the different testing conditions affecting failure, load frequency is one of the most detrimental features for composite specimens tested under fatigue loading due to the associated overheating that can produce undesirable degradation of the material properties. This issue has been and continues being, an ongoing fatigue topic. In this way, Chen and Hwang[32] and Marín et al.[33] have expounded the detrimental frequency effect on the fatigue performance of unidirectional composite laminates associated with the viscoelastic behavior of polymer matrix composites.

Due to the fact that damage in carbon/epoxy composite materials is more difficult to observe than in glass/epoxy composites, it is very useful to predict the onset and the progression of the transverse cracking on the 90° ply of a cross-ply laminate. As a good starting point, this initiation prediction can be reached using the *S–N* curve for UD-90 laminate as Hosoi et al.[16] expounded. Furthermore, Hashin and Rotem[34] established a fatigue failure

criterion from the *S–N* curves of 90° plies in material characterization, which may be useful as a first estimation of the fatigue damage density in a cross-ply laminate. Considering these two predictions, both the onset and the progression, as a first rough estimation, the definition of more complex experimental testing programs in which the authors are involved can be carried out. These more complex works are specifically focused on detecting the first transverse damage in the weakest ply of a laminate, that is, the 90° ply.

In this sense, the main objective of this work is to perform a profound fatigue life study of UD-90 laminates. To comprehend the fatigue performance of this type of composite material, several UD-90 configurations have been tested under different material features and testing conditions. In this way, four critical features for the UD 90° layer of multidirectional laminates to be subjected to fatigue testing have been identified and their effect is going to be analyzed; they are surface finishing, overheating due to high load frequency, porosity, and different plies thicknesses.

2 | EXPERIMENTAL PROGRAMS

Four test batches have been defined to analyze the effect of different conditions on the fatigue life of unidirectional 90° laminates. First, the existence of different external surface finishing in the samples has been analyzed to comprehend its effect on the fatigue life of this laminate type. Second, the effect of fatigue load frequency has been measured for all UD-90 laminates manufactured, assuring that the maximum thermal increment is lower than the allowed by the technical standard[35] in order to avoid a relevant degradation of their mechanical properties. Third, the effect of porosity level on the fatigue performance has been evaluated; the laminates have been cured in an autoclave at two different pressures, 3 and 7 bars, both of them are recommended by the manufacturer but for different applications (multidirectional laminate and sandwich, respectively), aiming to reach two different voids scenarios. And the last batch studied has been the significance of the prepreg thickness on the fatigue performance of the UD-90 laminates, manufacturing these laminates with different lamina grammages (including ultra-thin values) while a constant total thickness has been kept for them.

2.1 | Specimens' preparation

Aiming to assess the four case studies, two different raw materials have been used: the tape prepreg CYCOM 970/T300 of 190g/m^2 from Solvay and the tape prepreg TP 402/T700SC of 50g/m^2 from North Thin Ply Technology. Both materials have similar fiber percentages, 62% and 65%, respectively.

Three types of panels have been manufactured: a 3-bar conventional (3bC) panel and a 7-bar conventional (7bC) panel, both from the former raw material, and a 7-bar ultra-thin (7bUT) panel from TP 402/T700SC. In each case, the bar value indicated shows the work pressure for the autoclave curing. The curing process of all the panels has been carried out in an autoclave using a suitable vacuum bag.

Once cured, the fiber volume fraction of each laminate has been numerically measured using three different micrographs from each laminate, obtaining very similar values: 53.4% for 3bC samples, 55.2% for 7bC specimens, and 54.6% for the 7bUT panel.

After curing, E-glass fiber-reinforced tabs have been bonded ahead and behind at each side of the panels to prevent a premature failure, assuring the convenient gripping of the clamps during testing. Once the panels have been prepared, the specimens have been machined with a diamond disc. The dimensions selected have been $w = 25$ mm, $L_s = 180$ mm, $t = 2$ mm, and $L_t = 50$ mm, Figure 1, following the recommendations from technical standards.[35,36] The slightly reduced gauge length has been chosen after preliminary tests performed by the authors to optimize the material used and to economize the manufacturing process.

Although the 3-bar pressure is suggested by the manufacturer to cure sandwich laminates, it has been used here to cure a UD-90 laminate. Whereas 7bC samples have not shown any porosity, a small quantity of porosity has appeared on 3bC specimens' free edges as can be shown in Figure 2A; these specimens will be used to check if this scarce porosity value has a detrimental effect on the fatigue life. The quantity of porosity has been measured by means of an automatic image analysis, following TMS PT 2701 standard.[37] The results of this test show that a void percentage of 0.3% is found after the curing cycle at the lowest pressure indicated by the manufacturer. An inspected piece is presented in Figure 2B where the seven red marks correspond to voids.

In this way, to ensure that the 3bC panel has been accurately cured, two dynamic mechanical analysis (DMA) tests have been performed following ASTM D7028-07 standard[38]: one for the 3bC panel and another

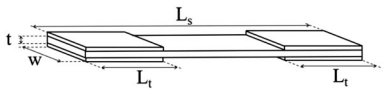

FIGURE 1 Specimen scheme with selected dimensions in mm.

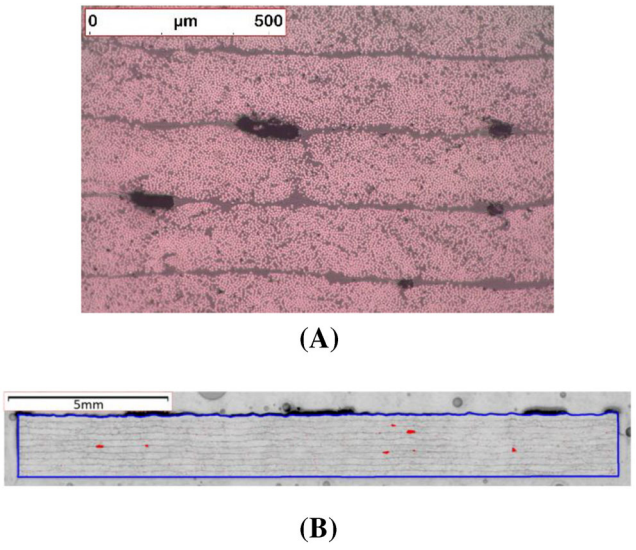

FIGURE 2 Porosity on 3bC sample free edge: (A) micrography in detail and (B) determination of the porosity content using automatic image analysis. [Colour figure can be viewed at wileyonlinelibrary.com]

for the 7bC. The results have shown that T_g onset is 181°C for 3bC and 185°C for 7bC, a difference that can be considered negligible to affect any mechanical property.

Due to the use of airweave in the vacuum bag, a rough surface is obtained in one of the sample's faces. To achieve a smooth finishing on both sample external surfaces, a pressure plate between the airweave and panels has been placed during the vacuum bag preparation. In order to avoid the inadequate extraction of air during curing, glass fiber yarns have been distributed along the laminate perimeter as paths to facilitate air extraction.

This change of finishing has been carried out to assess if the microscopic irregularities on the external sample surface due to the airweave may imply any stress concentrations that might be the potential nucleation point of a transverse crack.

2.2 | Test preparation

A significant number of tests have been carried out to analyze the four case studies proposed. On the one hand, static tension tests have been performed to evaluate both the elastic moduli and the tensile strength of each manufactured laminate. And, on the other hand, fatigue tension–tension (T–T) tests have been carried out to assess the fatigue life of each UD-90 laminate.

The static tests have been performed in an Instron 4482 electromechanical machine under displacement control at a speed of 0.5 mm/min. During testing a 2630-112/84 extensometer and/or HBM 1-LY41-6/120, strain gauges have been used to measure the strain and hence, the elastic moduli.

The cyclic tests have been carried out in an Instron 8801 hydraulic machine, controlling the load employing a sinusoidal function at a stress ratio $R = \sigma_{min}/\sigma_{max} = 0.1$. Different stress levels and load frequencies have been used to assess the fatigue life of the different laminates at room temperature. To ensure the viability of the use of the frequencies selected, a thermocouple has been fitted on the specimen surface to measure if relevant thermal increases exist on the specimens during fatigue testing. As ASTM D3479/D3479M standard[35] mentions, some material systems have demonstrated measurable degradation of material properties when suffering a 10°C increase; therefore, frequencies leading to thermal increase greater than this value will be discarded. The frequencies selected have been chosen following previous experiences from the authors' research group (Marín et al.[33]).

2.3 | Characterization

From each manufactured laminate, five samples have been quasi-statically tested to obtain both its tensile transverse strength, Y_T, and the corresponding elastic modulus, E_{22}. The results are shown in Table 1, including the standard deviation (SD) and the coefficient of variation (CV) for each mechanical property measured.

2.4 | Fatigue testing

In the first testing program 3bC samples have been tested at room temperature at two different frequencies, 10 and 15 Hz, under three different stress levels, 0.8, 0.7, and $0.65Y_T$; 19 samples being the total number of specimens tested. All tests have shown a maximum thermal increment of 5°C, lower than the 10°C defined limit. The fatigue life of the 3bC laminate is illustrated in Figure 3 employing *S*–*N* curves of different colors for each frequency tested.

In the second testing program, different 7bC laminates have been manufactured using a pressure plate as has been expounded in Section 2.1. Therefore, two different types of specimens have been obtained, rough and smooth samples, without using a pressure plate and using it, respectively. In what follows, the former is designated by R and the latter by S. The 7bC specimens have been tested at two different frequencies, 15 and 20 Hz, under three different stress levels, 0.8, 0.65, and $0.5Y_T$; 36 samples being the total number of specimens tested.

TABLE 1 Tensile transverse properties of each manufactured laminate.

	Y_T (MPa)	SD (MPa)	CV (%)	E_{22} (GPa)	SD (GPa)	CV (%)
3bC	69.07	±4.88	7.07	7.29	±0.07	0.97
7bC	73.16	±4.92	6.73	7.26	±0.21	2.88
7bUT	38.07	±6.32	16.59	7.58	±0.08	0.99

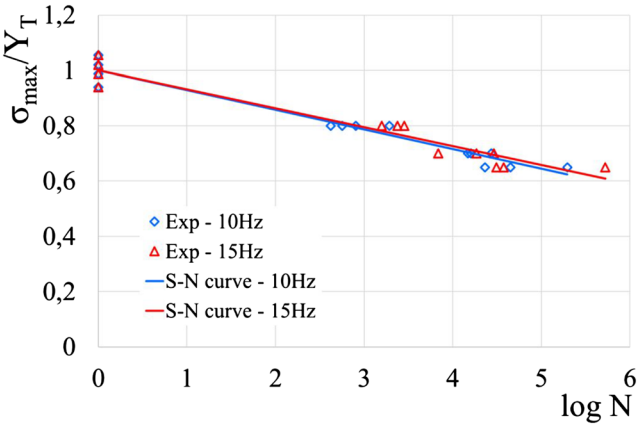

FIGURE 3 *S–N* curves of 3bC UD-90 samples (markers for experimental values) at 10 (blue) and 15 Hz (red). [Colour figure can be viewed at wileyonlinelibrary.com]

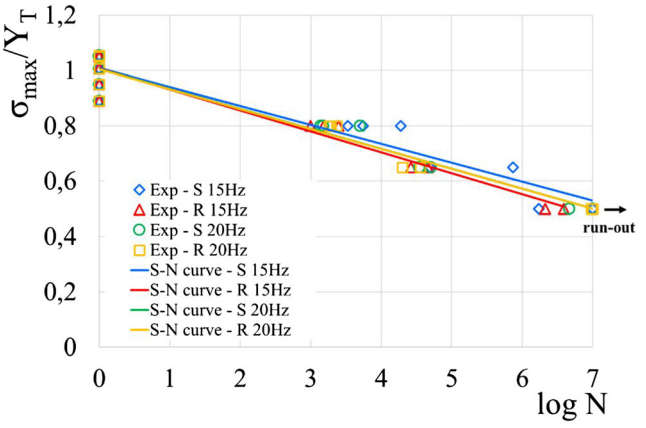

FIGURE 4 *S–N* curves of 7bC UD-90 samples (markers for experimental values) at 15 Hz for smooth (blue) and rough (red) samples and 20 Hz for smooth (green) and rough (yellow) samples. [Colour figure can be viewed at wileyonlinelibrary.com]

In this case, all tests have shown a maximum temperature increase of 7°C, also lower than the limit defined. In the same way as the previous program, the fatigue life of the 7bC laminate is illustrated in different colors employing *S–N* curves for each frequency and each surface finishing (Figure 4). In what follows, the *run-out* arrow indicates that there are specimens that have not failed after a certain number of cycles so the tests have been stopped at this point.

And, finally, the third experimental program has been performed to test the 7bUT laminate. The specimens have been tested at 15 Hz, under two different stress levels, 0.8 and 0.65Y_T; 18 samples being the total number of specimens tested. All the tests performed have shown a maximum thermal increase of 4°C, also below the limit defined. Figure 5 illustrates the fatigue life of the 7bUT laminate employing a *S–N* curve at the frequency tested.

To sum up, Table 2 shows a test matrix to summarize the experimental data generated in these three experimental programs. It is worth highlighting that the authors have employed two identical stress levels for the three case studies and a third different level between the conventional laminates in order to observe if the *S–N* curves obtained would be independent of this fact.

According to the fracture of UD-90 laminates, specimens are expected to fail after the appearance of the first transverse crack; a fact well corroborated after all the experimental programs. The sample has been divided

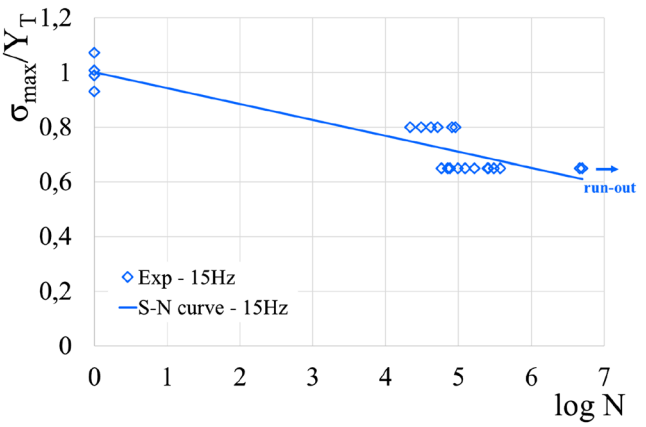

FIGURE 5 *S–N* curve of 7bUT UD-90 samples tested (markers for experimental values) at 15 Hz. [Colour figure can be viewed at wileyonlinelibrary.com]

into three different fracture zones in which the transverse crack may appear: A zone of 10 mm from one tab, C zone of 10 mm from the other tab, and B zone of 60 mm between the two other zones. Two of them, A and C, are the areas close to the tabs and the B zone is the regularized one.

In order to analyze the differential behavior of each laminate, the experimental occurrence percentage of the transverse crack according to the different fracture zones has been measured. 3bC samples have shown a 73.7% of

TABLE 2 Test matrix summarizing the experimental programs performed, indicating the number of specimens tested under fatigue loading for each study case.

Laminate	Prepreg grammage	Porosity	Surface finishing	Frequency (Hz)			Stress levels (σ_{max}/Y_T)
				10	15	20	
3bC	CONV	YES	R	10	9	-	0.8, 0.7, 0.65
7bC	CONV	NO	R	-	9	9	0.8, 0.65, 0.5
	CONV	NO	S	-	9	9	0.8, 0.65, 0.5
7bUT	UT	NO	R	-	18	-	0.8, 0.65

their fractures in the B zone, 7bC a 52.8%, and 7bUT has only shown a 22.2%. It is worth pointing out that for most laminates more than half of the specimens failures have occurred in the regularized zone whereas it might be expected the opposite situation, or even the occurrence in the tabs, due to the stress concentrations promoted by the geometry of the tabs.

As it has been detailed, the highest number of occurrences has appeared in the regularized zone, B zone, except for 7bUT samples (although the manufacturing process has been identical in all cases). Therefore, the results of this laminate at $0.65Y_T$ presented in Figure 5 should be analyzed from this perspective.

3 | RESULTS AND DISCUSSIONS

Each effect considered as one case study has been analyzed independently. However, to describe the fatigue data in view of the analysis of the results, the *S–N* curves have been shown at the same time that every experimental testing program has been presented. It is a well-known fact that there are many different forms of *S–N* equations, which can be a linear curve on a log–log or semi-log plot. In this case, the next linear law is assumed for a semi-log chart:

$$\frac{\sigma_{max}}{Y_T} = k - m \log N, \quad (1)$$

where σ_{max} is the maximum stress level in the cyclic test, Y_T is the ultimate strength of the material (particularly, the tensile transverse strength), N is the total cycle of fatigue life, and k and m are material parameters obtained by regression methods. These *S–N* curve parameters are shown in Table 3 for each case study.

Furthermore, a statistic fitting analysis has been performed. After obtaining the *S–N* curve parameters needed, *R*-squared (R^2) has been calculated to indicate if the regression model adequately fits the experimental data. Although R^2 is a slight estimation of the goodness-of-fit measure, this statistic variable has been obtained to give an indication of the variability of the results. The R^2 values have been also shown in Table 3.

TABLE 3 *S–N* curves parameters and the R^2 for fatigue life data of each experimental program.

Case study	k	m	R^2
3bC 10 Hz	0.9997	0.0710	0.9568
3bC 15 Hz	1.0011	0.0686	0.9386
7bC 15 Hz Smooth	1.0094	0.0685	0.9411
7bC 15 Hz Rough	1.0073	0.0759	0.9078
7bC 20 Hz Smooth	1.0063	0.0723	0.9399
7bC 20 Hz Rough	1.0045	0.0720	0.9393
7bUT 15 Hz	1.0016	0.0584	0.8180

As can be observed, the R^2 values for the 3bC cases are very similar to the 7bC cases, all of them being close to 1. The remainder dispersion may be due to the variability of the transverse strength to the fiber direction. From the 7bC cases, 7bC 15 Hz Smooth has more dispersion than the rest of them and hence, its R^2 is smaller. The dispersion of the 7bUT case is remarkable due to the variability of fractures of ultra-thin 90° laminates at $0.65Y_T$ already mentioned and quantified at the end of Section 2.4. Nevertheless, its R^2 continues being quite satisfactory from a statistical viewpoint.

In addition to this statistic parameter, the 95% confidence and prediction levels are going to be plotted for the different study cases in the following sections. These two probability intervals have been calculated using the Student's *t*-distribution with $n - 2$ degrees of freedom, taking a sample of n observations.

The interest of these statistical intervals has been related to the definition of more complex experimental programs on cross-ply laminates (see Sánchez-Carmona et al.[39]). In this recently published work, the authors have microscopically looked for the onset of transverse damages which appears in the weakest layer in cross-ply laminates, the 90° one. After certain stops performed at

different numbers of cycles, the main part of this work has been the microscopic inspections of the 90° layer using an optical microscope. As has also been discussed in the last paragraph of the introduction section, the first transverse crack in a cross-ply laminate can be predicted using the unidirectional fatigue life. For that reason, knowing the confidence levels around the average of the *S–N* curve and the maximum and minimum values that can be obtained (prediction levels), the first transverse damage predictions can be calculated in a secure interval. Taking the lower and the upper unidirectional fatigue lives into consideration, an estimative cycle range at which the first transverse damage may appear can be predicted. In that way, the microscopic inspection stops are done in a secure interval to avoid missing the first transverse damages that could appear in the 90° layer.

3.1 | Effect of surface finishing

Although the scattering for unidirectional laminates under fatigue testing is expected to be high, the microscopic observations of the specimens fractured seem to show that the failures of UD-90 samples occur at some irregular areas which are created by the rough texture of one surface of the laminate due to airweave used in the manufacturing process (Figure 6). These irregularities seem to be potential stress concentrators for the fracture of the UD-90 samples. In order to analyze this issue, 7bC laminates have been manufactured using a pressure plate as has been previously explained.

The results for the fatigue life of the second experimental program have been already shown in Figure 4. Considering each frequency case for the 7bC laminate separately, rough external surface finishing at 15 Hz seems to move the *S–N* curve slightly to the left, which means that fractures of the UD-90 laminate may occur prematurely due to the roughness of the surface finishing provoked by the airweave; otherwise, the *S–N* curves at 20 Hz are overlapped.

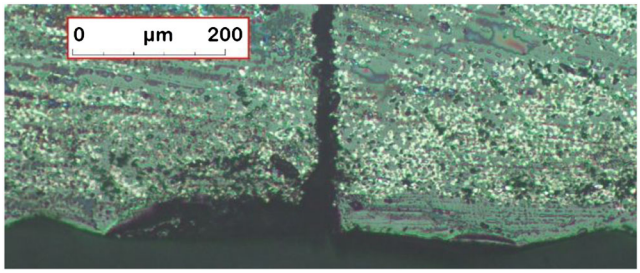

FIGURE 6 Cracks in UD-90 samples occurring at irregular areas due to the rough surface of this laminate. [Colour figure can be viewed at wileyonlinelibrary.com]

Therefore, observing all the results together in Figure 4 and taking into consideration the scattering of fatigue life for composite materials, the roughness of the external surface finishing can be neglected as the promoter for the premature fracture of UD-90 laminates.

Taking into account this last assumption, the *S–N* curves from Figure 4 are going to be reduced to only two trends, one at each frequency tested as is shown in Figure 7. In this way, the values for the *S–N* curves and their R^2 are shown in Table 4.

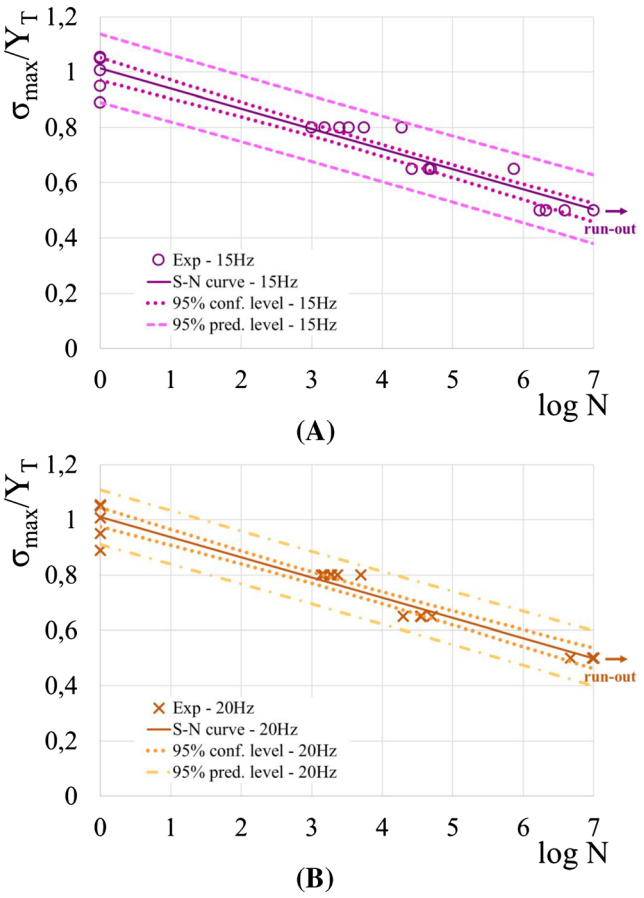

FIGURE 7 *S–N* curve of 7bC UD-90 samples tested (markers for experimental values) and the 95% confidence and prediction levels at (A) 15 and (B) 20 Hz. [Colour figure can be viewed at wileyonlinelibrary.com]

TABLE 4 *S–N* curves values and associated statistics for fatigue life data of the 7bC laminate.

Case study	*k*	*m*	R^2
7bC 15 Hz	1.0139	0.0729	0.9215
7bC 20 Hz	1.0097	0.0729	0.9494

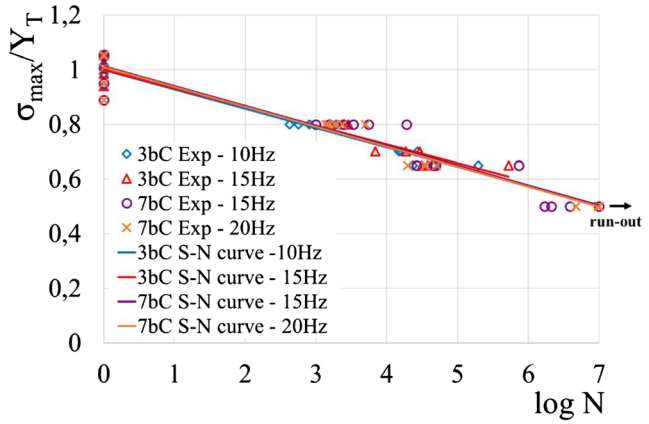

FIGURE 8 Comparison of *S–N* curves obtained at all frequencies tested in each experimental testing program. [Colour figure can be viewed at wileyonlinelibrary.com]

3.2 | Effect of frequency

Different frequencies have been used in the experimental programs for 3bC and 7bC laminates. The main objective has been to identify the highest frequency allowed to perform the tests in the quickest way, without producing an out-of-limit thermal increase. In this sense and as has been shown in the previous section, none of the frequencies used has implied an increment of 10°C; particularly, the highest measurement has been 7°C at 20 Hz.

All *S–N* curves from 3bC and 7bC specimens have been charted together in Figure 8. On the one hand, 3bC samples have shown very similar *S–N* curves at both frequencies tested in the first fatigue program. Conversely, it is worth pointing out that the dispersion of experimental data at 15 Hz and $0.65Y_T$ has produced a slight reduction of R^2 (Table 3). Although this statistic value is lower than that associated with 10 Hz, both frequencies, 10 and 15 Hz, have given rise to equivalent test results in UD-90 laminates. And, on the other hand, the experimental fatigue life of each frequency of the second program for 7bC samples can be also observed in Figure 8. In this case, the scatter of the results has been slightly lower than in the case of the 3bC samples as can be concluded from Tables 3 and 4.

Therefore, all frequencies tested can be employed to define the fatigue life of UD-90 laminates due to the similarity of all *S–N* curves obtained, reaching a common *S–N* curve and their statistic parameters as can be seen in Figure 9. Moreover, Table 5 shows the values for this unique *S–N* curve.

After all conventional results have been combined to obtain a unique *S–N* curve, the use of different stress levels in the conventional laminates has verified that a higher or lower stress level is independent of obtaining a good *S–N* curve.

3.3 | Effect of voids

Taking into account that the existence of porosity is scarce after curing at any pressure in the interval given by the manufacturer, the fatigue life of both laminates, 3bC and 7bC, is similar if we compare the *S–N* curves calculated at any frequency tested, as Figure 8 shows. Hence, the existence of a few voids, 0.3% or less, has a negligible effect on the fatigue performance of UD-90 samples.

3.4 | Effect of ply thickness

Before starting to analyze the effect of ply thickness, it is important to remember that the damage in a 90° layer of a composite laminate is dominated by fiber/matrix debonding. Hence, the development of the crack is produced through the fiber/matrix interfaces and not exclusively along the matrix. This idea is illustrated by the micrograph shown in Figure 10.

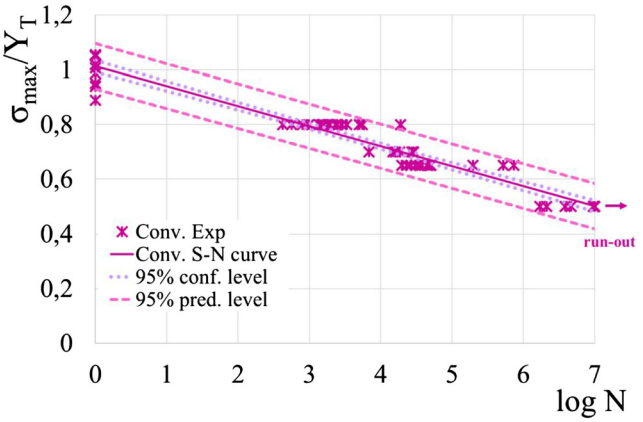

FIGURE 9 *S–N* curve and the 95% confidence and prediction levels for conventional material specimens at any frequency tested. [Colour figure can be viewed at wileyonlinelibrary.com]

TABLE 5 *S–N* curve values and associated statistics for fatigue life data of the conventional laminates at any frequency tested.

Case study	*k*	*m*	R^2
3bC and 7bC at any *f*	1.0132	0.0731	0.9350

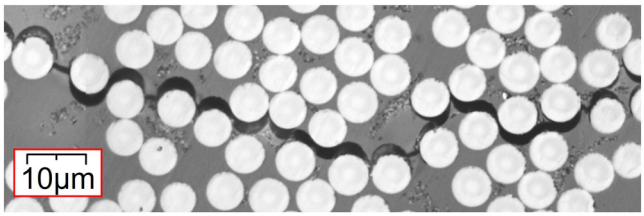

FIGURE 10 Fiber/matrix debonding in a 90° layer. [Colour figure can be viewed at wileyonlinelibrary.com]

As Table 2 summarizes, three different UD-90 laminates have been tested under cyclic loading, two of them are made of conventional prepreg (3bC and 7bC) and the other one of ultra-thin material. After checking that the previous effects (surface roughness, load frequency, and a scarce void content) are negligible for the fatigue life of UD-90 samples, the experimental data for conventional material (Figure 9) are going to be compared with the obtained for UT UD-90 samples (Figure 5).

The conventional and ultra-thin materials employed are not composed of the same fibers and resin; hence, the *S–N* curves for both types of materials (conventional and ultra-thin) have also been plotted using the dimensionless stress level (divided by Y_T), Figure 11A. In this chart, it can be observed that the fatigue life of the UTP laminate has reached one order of magnitude higher at high cycle fatigue loading. It is worth mentioning that these results seem to be in accordance with the expected fact if both prepregs were made of the same fibers and resin. Specifically, according to the physically based explanation of the scale effect in composite laminates involving UTP prepregs, París et al.,[28] the transverse damage is delayed when ultra-thin plies are involved.

Furthermore, Figure 11B, represented as the maximum ultimate tensile stress versus the number of cycles, shows how the slope for conventional UD-90 samples is higher than for the ultra-thin ones, implying an improvement in the fatigue life of the ultra-thin UD-90 laminate.

Additionally, the improvement of fatigue life may also be explained due to the different microstructure of the samples (Figure 12), discriminating between conventional and ultra-thin prepregs, and considering the different pattern for the appearance of transverse damage when ultra-thin plies are involved as París et al.[28] detailed. Whereas 3bC and 7bC have been manufactured using just 10 plies, 7bUT has been performed using 36 plies to achieve the same laminate thickness. This fact implies a different microstructure between laminates, showing more local resin-rich areas between plies in the 7bUT laminate. These resin-rich areas may act as barriers

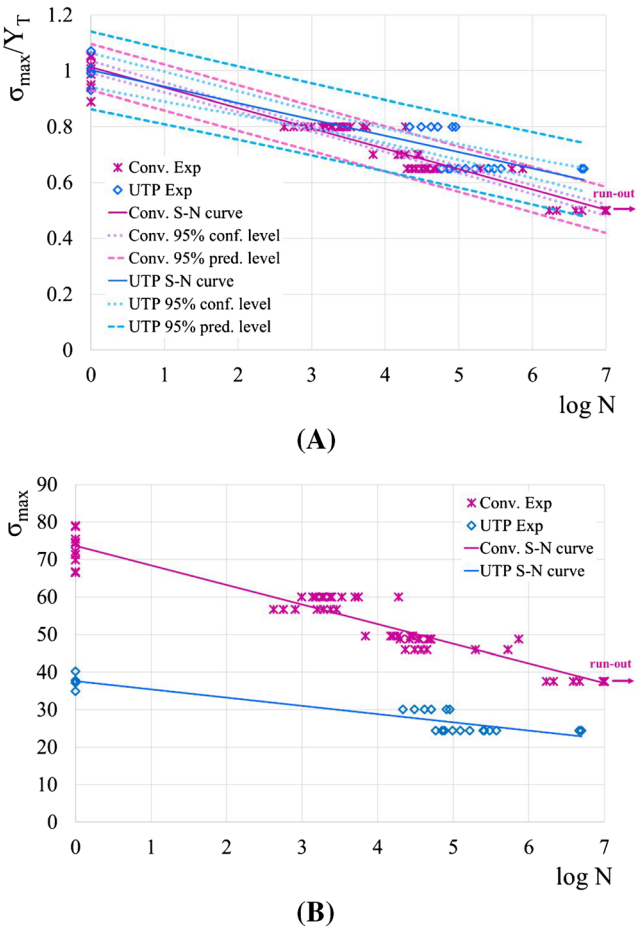

FIGURE 11 Comparison of *S–N* curves obtained: (A) S being the dimensionless maximum stress and (B) S being the maximum stress, for which the 95% confidence and prediction levels for conventional (Conv.) and ultra-thin (UTP) UD-90 laminate are shown. [Colour figure can be viewed at wileyonlinelibrary.com]

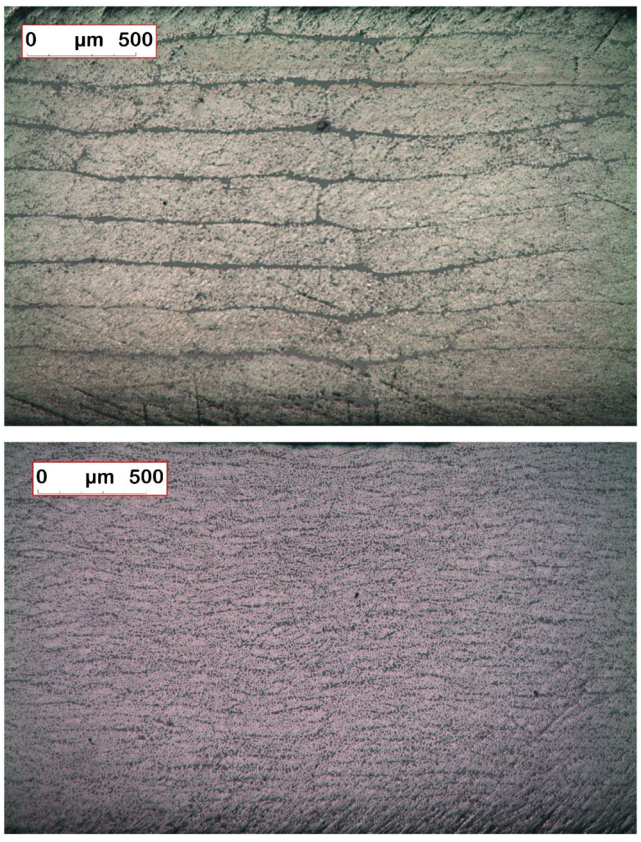

FIGURE 12 Microstructures at the same magnification for (A) 7bC and (B) 7bUT. [Colour figure can be viewed at wileyonlinelibrary.com]

which slow down the fiber/matrix debonding advance. The same fact is discussed by Galos[31] in the review done for ultra-thin plies.

4 | CONCLUSIONS

The main objective of this paper has been to measure the fatigue life of different UD-90 laminates under different manufacturing and testing conditions. Taking the fatigue life trendlines and the statistical analysis into account, the following conclusions have been obtained. First, a void content below 0.3% has a negligible effect on fatigue life. Hence, the whole pressure range indicated by the manufacturer between both pressure limits (depending on the use of the raw material either in a sandwich panel or in a laminate) is acceptable. Second, sample surface topology (using either airweave or a flat metal plate) does not significantly influence the fatigue life. Third, UD-90 laminates can be tested up to 20 Hz at room temperature without overheating and thus avoiding the undesirable degradation of fatigue properties. Finally, an improvement in fatigue performance of UD-90 samples has been found when 50g/m^2 prepreg is used, obtaining a lower *S–N* curve slope independently of the way of representing the stress level in the vertical axis.

The results have led to conclude that the fatigue life of UD-90 laminates has been accurately defined employing semi-log *S–N* curves. Fatigue performance of this type of unidirectional composite material can be assessed under different possible conditions without losing reliability and accuracy, economizing the time and the auxiliary material used in cyclic tests. These results are relevant for the authors' current studies on the fatigue behavior of ultra-thin laminas in cross-ply laminates to understand the *scale effect*.

ACKNOWLEDGMENTS

This work was supported by the Universidad de Sevilla (Grant VIPPIT-2018-II.2), Consejería de Economía y Conocimiento, Junta de Andalucía (project number P18-FR-3360) corresponding to the I+D+I Programa Operativo FEDER 2014-2020, and Spanish Ministry of Science, Innovation and Universities (project number PID2021-126279OB-I00). The authors appreciate Dr. Jesús Justo Estebaranz for their advice according to the frequency issue during the definition of fatigue tests.

DATA AVAILABILITY STATEMENT

The raw/processed data required to reproduce these findings cannot be shared at this time as the data also forms part of an ongoing study.

ORCID

Serafín Sánchez-Carmona https://orcid.org/0000-0002-8640-5644

REFERENCES

1. Harris B (Ed). *Fatigue in Composites*. Woodhead Publishing; 2003. doi:10.1533/9781855738577
2. Murri GB. Evaluation of delamination onset and growth characterization methods under mode I fatigue loading. In: *27th Annual Technical Conference of the American Society for Composites 2012, Held Jointly with 15th Joint US-Japan Conference on Composite Materials and ASTM-D30 Meeting*. Destech Publications; 2013.
3. Pupurs A, Varna J. Energy release rate based fiber/matrix debond growth in fatigue. Part I: self-similar crack growth. *Mech Adv Mater Struct*. 2013;20(4):276-287. doi:10.1080/15376494.2011.627627
4. Pupurs A, Krasnikovs A, Varna J. Energy release rate based fiber/matrix debond growth in fatigue. Part II: Debond growth analysis using Paris law. *Mech Adv Mater Struct*. 2013;20(4):288-296. doi:10.1080/15376494.2011.627628
5. Schorer N, Sause MGR. Identification of failure mechanisms in CFRP laminates using 3D digital image correlation. In: *ICCM International Conferences on Composite Materials*. Vol.2015; 2015:19-24.
6. Llobet J, Maimí P, Mayugo JA, Essa Y, Martin de la Escalera F. A fatigue damage and residual strength model for unidirectional carbon/epoxy composites under on-axis tension-tension loadings. *Int J Fatigue*. 2017;103:508-515. doi:10.1016/j.ijfatigue.2017.06.026
7. Rubiera S, Argüelles A, Viña J, Rocandio C. Study of the phenomenon of fatigue delamination in a carbon-epoxy composite under mixed mode I/II fracture employing an asymmetric specimen. *Int J Fatigue*. 2018;114(May):74-80. doi:10.1016/j.ijfatigue.2018.05.015
8. Boniface L, Ogin SL. Application of the Paris equation to the fatigue growth of transverse ply cracks. *J Compos Mater*. 1989; 23(7):735-754. doi:10.1177/002199838902300706
9. Lafarie-Frenot MC, Henaff-Gardin C. Formation and growth of 90° ply fatigue cracks in carbon/epoxy laminates. *Compos Sci Technol*. 1991;40(3):307-324.
10. Henaff-Gardin C, Lafarie-Frenot MC. Fatigue behaviour of thermoset and thermoplastic cross-ply laminates. *Composites*. 1992;23(2):109-116.
11. Song DY, Otani N. Fatigue life prediction of cross-ply composite laminates. *Mater Sci Eng A*. 1997;238(2):329-335.
12. Gamstedt EK, Sjögren BA. Micromechanisms in tension-compression fatigue of composite laminates containing transverse plies. *Compos Sci Technol*. 1999;59(2):167-178.
13. Berthelot JM, Le Corre JF. Modelling the transverse cracking in cross-ply laminates: Application to fatigue. *Compos Part B Eng*. 1999;30(6):569-577.
14. Taheri-Behrooz F, Shokrieh MM, Lessard LB. Residual stiffness in cross-ply laminates subjected to cyclic loading. *Compos Struct*. 2008;85(3):205-212.
15. Tohgo K, Nakagawa S, Araki H. Damage behavior and life prediction in CFRP cross-ply laminates under fatigue loading. *Nihon Kikai Gakkai Ronbunshu, A Hen/Trans Japan Soc Mech Eng Part A*. 2006;72(7):1041-1048.

16. Hosoi A, Sakuma S, Fujita Y, Kawada H. Prediction of initiation of transverse cracks in cross-ply CFRP laminates under fatigue loading by fatigue properties of unidirectional CFRP in 90° direction. *Compos Part A Appl Sci Manuf*. 2015;68:398-405.
17. Carraro PA, Maragoni L, Quaresimin M. Characterisation and analysis of transverse crack-induced delamination in cross-ply composite laminates under fatigue loadings. *Int J Fatigue*. 2019; 129(August):105217
18. Llobet J, Maimí P, Essa Y, Martin de la Escalera F. Progressive matrix cracking in carbon/epoxy cross-ply laminates under static and fatigue loading. *Int J Fatigue*. 2019;119(October 2018):330-337.
19. Hahn HT, Lorenzo L. Fatigue Failure Mechanisms in Composite Laminates. International Congress on Fracture (ICF); 1984.
20. Lafarie-Frenot MC, Rouquie S. Influence of oxidative environments on damage in carbon/epoxy laminates subjected to thermal cycling. *Compos Sci Technol*. 2004;64(10–11):1725-1735.
21. Lafarie-Frenot MC, Ho NQ. Influence of free edge intralaminar stresses on damage process in CFRP laminates under thermal cycling conditions. *Compos Sci Technol*. 2006;66(10):1354-1365.
22. Sihn S, Kim RY, Kawabe K, Tsai SW. Experimental studies of thin-ply laminated composites. *Compos Sci Technol*. 2007;67(6): 996-1008.
23. Amacher R, Cugnoni J, Botsis J, Sorensen L, Smith W, Dransfeld C. Thin ply composites: Experimental characterization and modeling of size-effects. *Compos Sci Technol*. 2014; 101:121-132.
24. Quaresimin M, Carraro PA, Mikkelsen LP, et al. Damage evolution under cyclic multiaxial stress state: A comparative analysis between glass/epoxy laminates and tubes. *Compos Part B Eng*. 2014;65:2-10.
25. Sisodia S, Gamstedt EK, Edgren F, Varna J. Effects of voids on quasi-static and tension fatigue behaviour of carbon-fibre composite laminates. *J Thermoplast Compos Mater*. 2015;49(17): 2137-2148.
26. Wagner P, Schwarzhaupt O, May M. In-situ X-ray computed tomography of composites subjected to fatigue loading. *Mater Lett*. 2019;236:128-130.
27. El-Dessouky HM, Lawrence CA. Ultra-lightweight carbon fibre/thermoplastic composite material using spread tow technology. *Compos Part B Eng*. 2013;50:91-97.
28. París F, Velasco ML, Correa E. The scale effect in composites: An explanation physically based on the different mechanisms of damage involved in failure. *Compos Struct*. 2021;257:113089
29. París F, Velasco ML, Correa E. Chapter 9: Modelling fibre–matrix interface debonding and matrix cracking in composite laminates. Multi-Scale Contin Mech Model Fibre-Reinforced Polym Compos. Published online January 1, 2021:243–274.
30. Kötter B, Endres J, Körbelin J, Bittner F, Endres HJ, Fiedler B. Fatigue and fatigue after impact behaviour of Thin- and Thick-Ply composites observed by computed tomography. *Compos Part C Open Access*. 2021;5(March):100139
31. Galos J. Thin-ply composite laminates: a review. *Compos Struct*. 2020;236(September 2019):111920. doi:10.1016/j.compstruct.2020.111920
32. Chen HS, Hwang SF. Accelerated fatigue properties of unidirectional carbon/epoxy composite materials. *Polym Compos*. 2006;27(2):138-146.
33. Marin JC, Justo J, París F, Cañas J. The effect of frequency on tension-tension fatigue behavior of unidirectional and woven fabric graphite-epoxy composites. *Mech Adv Mater Struct*. 2019; 26(17):1430-1436.
34. Hashin Z, Rotem A. A fatigue failure criterion for fiber reinforced composite laminae. *J Thermoplast Compos Mater*. 1973; 7:448-464.
35. ASTM D3479/D3479M: Standard Test Method for Tension-Tension Fatigue of Polymer Matrix Composite Materials. Annu B ASTM Stand. 2012;96(August):6.
36. ASTM D3039/D3039M: Standard Test Method for Tensile Properties of Polymer Matrix Composite Materials. Annu B ASTM Stand. Published online 2014:1–13.
37. TMS PT 2701: Determinación del contenido de poros en plásticos reforzados con fibras usando Análisis Automático de Imágenes.
38. ASTM D7028–07: Standard Test Method for Glass Transition Temperature (DMA Tg) of Polymer Matrix Composites by Dynamic Mechanical Analysis (DMA). Annu B ASTM Stand. Published online 2012:1–14.
39. Sánchez-Carmona S, Correa E, Barroso A, París F. Experimental observations of fatigue damage in cross-ply laminates using carbon/epoxy ultra-thin plies. *Compos Struct*. 2023;306 (116564):116564

How to cite this article: Sánchez-Carmona S, Correa E, Barroso A, París F. Fatigue life of unidirectional 90° carbon/epoxy laminates made of conventional and ultra-thin plies varying manufacturing and testing conditions. *Fatigue Fract Eng Mater Struct*. 2023;1-11. doi:10.1111/ffe.13966